Med Chem Res (2017) 26:615–630
DOI 10.1007/s00044-017-1782-4

MEDICINAL CHEMISTRY RESEARCH

ORIGINAL RESEARCH

Synthesis, characterization, preliminary SAR and molecular docking study of some novel substituted imidazo[2,1-*b*][1,3,4]thiadiazole derivatives as antifungal agents

Mustafa Er[1] · Buğracan Ergüven[2] · Hakan Tahtaci[3] · Abdurrahman Onaran[4] · Tuncay Karakurt[5] · Abdulilah Ece[6]

Received: 23 April 2016 / Accepted: 4 January 2017 / Published online: 12 January 2017

Abstract The aim of this study was to synthesize imidazo[2,1-*b*][1,3,4]thiadiazole derivatives, characterize them with various spectroscopic methods and investigate their antifungal activities. 2-Amino-1,3,4-thiadiazole derivatives **2a, b** were synthesized by reacting nitrile compounds **1a, b** with thiosemicarbazide (yields 75 and 88%). We then synthesized imidazo[2,1-*b*][1,3,4]thiadiazole derivatives **4–21**, the target compounds, from the reactions of 2-amino-1,3,4-thiadiazole derivatives **2a, b** with phenacyl bromide derivatives **3** (yields 52–69%). The structures of all synthesized compounds were characterized by infrared, ^{1}H nuclear magnetic resonance, ^{13}C nuclear magnetic resonance, elemental analysis and mass spectroscopy and X-ray diffraction analysis was also used for the compounds **7, 8, 10,** and **17**. Subsequently, in vitro antifungal activity tests were applied to all synthesized compounds. Inhibition zones, percentages of inhibition and LD50 doses were determined. Most of the synthesized compounds exhibited good antifungal activity against plant pathogens. Molecular docking and electronic properties calculations were carried out in order to see the potential binding conformations of the ligands and the effect of the substituents on the activities. Docking score successfully reflects the activity of the most active compound **10**, which was found to have the lowest octanol/water partition coefficient and high HOMO energy value. The combination of experimental and computational work show that all the synthesized compounds have promising activities and might serve as novel drug candidates.

Keywords 2-Amino-[1,3,4]thiadiazole · Imidazo[2,1-*b*][1,3,4]thiadiazole · Phenacyl bromide · Molecular docking · Antifungal activity · SAR

Electronic supplementary material The online version of this article (doi:10.1007/s00044-017-1782-4) contains supplementary material, which is available to authorized users.

✉ Mustafa Er
mustafaer@karabuk.edu.tr

[1] Department of Chemical Engineering, Faculty of Engineering, Karabuk University, Karabuk 78050, Turkey

[2] Department of Chemistry, Faculty of Science, Karabuk University, Karabuk 78050, Turkey

[3] Department of Polymer Engineering, Faculty of Technology, Karabuk University, Karabuk 78050, Turkey

[4] Department of Plant Protection, Faculty of Agriculture, Gaziosmanpasa University, Tokat 60250, Turkey

[5] Department of Chemical Engineering, Faculty of Engineering and Architecture, Ahi Evran University, Kırşehir 40100, Turkey

[6] Department of Pharmaceutical Chemistry, Faculty of Pharmacy, Biruni University, Istanbul 34010, Turkey

Introduction

Despite the recent significant increase in the discovery of compounds with antimicrobial activities, the use of these compounds remains rather limited due to the difficulties of application, high risks of toxicity, drug resistance, undesired side effects, pharmacokinetic deficiencies and/or inadequate antimicrobial activities. Hence, synthetic organic chemists have been interested in developing biological active compounds with minimal side effects.

Imidazole and 1,3,4-thiadiazole are well known heterocyclic compounds widely used in pharmaceutical chemistry (Kim et al. 2013; Padmavathi et al. 2011; Singh et al. 2016; El-Gohary and Shaaban 2013). The synthesis and

characterization of imidazole and 1,3,4-thiadiazole derivatives having various biological activities are still being investigated today (Banu et al. 2010; Romagnoli et al. 2015; Kamal et al. 2014). These heterocyclic systems in which imidazole and 1,3,4-thiadiazole rings are fused together with a bridgehead nitrogen atom are referred to as imidazo [2,1-*b*][1,3,4]thiadiazoles (Alwan et al. 2015).

Imidazo[2,1-*b*][1,3,4]thiadiazoles and their heterocyclic derivatives are known to exhibit several biological activities, including antibacterial (Luo et al. 2013; Chandrakantha et al. 2014; Atta et al. 2011), antifungal (Lata et al. 2015), antimicrobial (Lamani et al. 2009; Alegaon and Alagawadi 2011), anti-inflammatory (Kadi et al. 2007; Gadad et al. 2008; Jadhav et al. 2008), and antituberculosis (Ramprasad et al. 2015; Alegaon et al. 2012) activities. Being a bio-isostere of Levamisole (which is used to regulate and strengthen the immune system), these compounds have attracted many researchers studying anticancer activities (Tegginamath et al. 2013; Patel et al. 2015; Noolvi et al. 2011; Terzioglu and Gursoy 2003; Noolvi et al. 2012; Kumar et al. 2014; Karki et al. 2011). In addition, several studies conducted with imidazo[2,1-*b*][1,3,4]thiadiazoles and their derivatives reported that these compounds was being used in various industries, such as dye, herbicide and insecticide production (Bakherad et al. 2010; Jalhan et al. 2012). Hence, imidazo[2,1-*b*][1,3,4]thiadiazoles and derivatives have become important members of the heterocyclic compounds in pharmaceutical chemistry.

The most commonly used method to synthesize imidazo [2,1-*b*][1,3,4]thiadiazole derivatives is the reaction of 2-amino-1,3,4-thiadiazole derivatives with appropriate phenacyl bromide derivatives (Tzitzikas et al. 2013). However, a new method known as Suzuki-Miyaura cross-coupling reactions has recently been used to synthesize these compounds (Copin et al. 2012; Kotha et al. 2002).

In the light of the aforementioned literature survey, the aims of this study include the following: the synthesis of imidazo[2,1-*b*][1,3,4]thiadiazole derivatives with potential biological activities; the characterization of these compounds with various spectroscopic methods; and the investigation of in vitro antifungal activity. The computational studies were also utilized to gain insight into the binding mode of the compounds and the effect of substituents on the activities. The synthetic method used to synthesize these compounds is shown below in Scheme 1.

Results and discussion

Chemistry

In the first part of the study, we synthesized 2-amino-1,3,4-thiadiazole derivatives **2a, b** from the reactions of nitrile compounds **1a, b** with thiosemicarbazide in trifluoroacetic acid (TFA) at 60 °C with high yields (75 and 88%). 2-Amino-1,3,4-thiadiazole derivatives **2a, b** were obtained as specified in the literature (Er et al. 2014; Er et al. 2016).

In the infrared (IR) spectra of 2-amino-1,3,4-thiadiazole derivatives **2a, b**, two peaks were observed at 3265, 3088 cm^{-1} which corresponding to the symmetric and asymmetric absorption bands of $-NH_2$ group.

The structures of 2-amino-1,3,4-thiadiazole derivatives **2a, b** were confirmed by ^1H NMR spectroscopy, as well. In the ^1H nuclear magnetic resonance (NMR) spectra, the proton signals of -NH_2 group in **2a, b** which bonded to the 1,3,4-thiadiazole ring at the C-2 position were recorded as a singlet in the range between 7.04–7.09 ppm corresponding to two protons. Proton peaks belonging to the -NH_2 group of these compounds **2a, b** disappeared as a result of the proton-deuterium exchange performed with D_2O. The methylene ($-CH_2$) protons bonding the thiophene and phenyl groups to the thiadiazole ring at the 5-position were observed as a singlet corresponding to two protons in the range between 4.02–4.36 ppm.

The structures of 2-amino-1,3,4-thiadiazole derivatives **2a, b** were also confirmed by the ^{13}C NMR spectrum. C-2 carbon signals of the 2-amino-1,3,4-thiadiazole ring in these compounds were recorded in the range between 159.07, 157.57 ppm, and C-5 carbon signals were recorded in the range between 169.75, 169.44 ppm. In the ^{13}C NMR spectra, it was observed that the resonance values of carbons at the C-2 and C-5 positions of the 2-amino-1,3,4-thiadiazole ring were highly compatible with these types of compounds in the literature (Sancak et al. 2007). Other spectral data pertaining to the carbon skeleton of the compounds fully support the suggested structures. Experimental part, the physical properties and the spectral data related to compounds **2a, b** are provided in detail in the Supplementary Material Section.

In the second part of this study, we synthesized imidazo [2,1-*b*][1,3,4]thiadiazole derivatives **4–21**, the target compounds, by the reactions of 2-amino-1,3,4-thiadiazole derivatives **2a, b** with phenacyl bromide derivatives **3** in absolute ethyl alcohol with moderate-high yields (52–69%) (Scheme 1). According to the IR spectral data, -NH_2 symmetric and asymmetric absorption bands of the compounds **2a, b** observed at 3265, 3088 cm^{-1} were disappeared for the compounds **4–21.** This IR data demonstrates the most important evidence for the formation of imidazo[2,1-*b*] [1,3,4]thiadiazole derivatives **4–21**.

Also, the -NH_2 group proton signals observed in the 7.04–7.09 ppm range disappeared in the 2-amino-1,3,4-thiadiazole derivatives which were the precursors of imidazo[2,1-*b*][1,3,4]thiadiazole derivatives **4–21** in the ^1H NMR spectra. Instead, a singlet was observed that corresponds to one proton in the 8.48–8.94 ppm range

Scheme 1 Synthesis of substituted imidazo[2,1-*b*][1,3,4]thiadiazole derivatives **4-21**

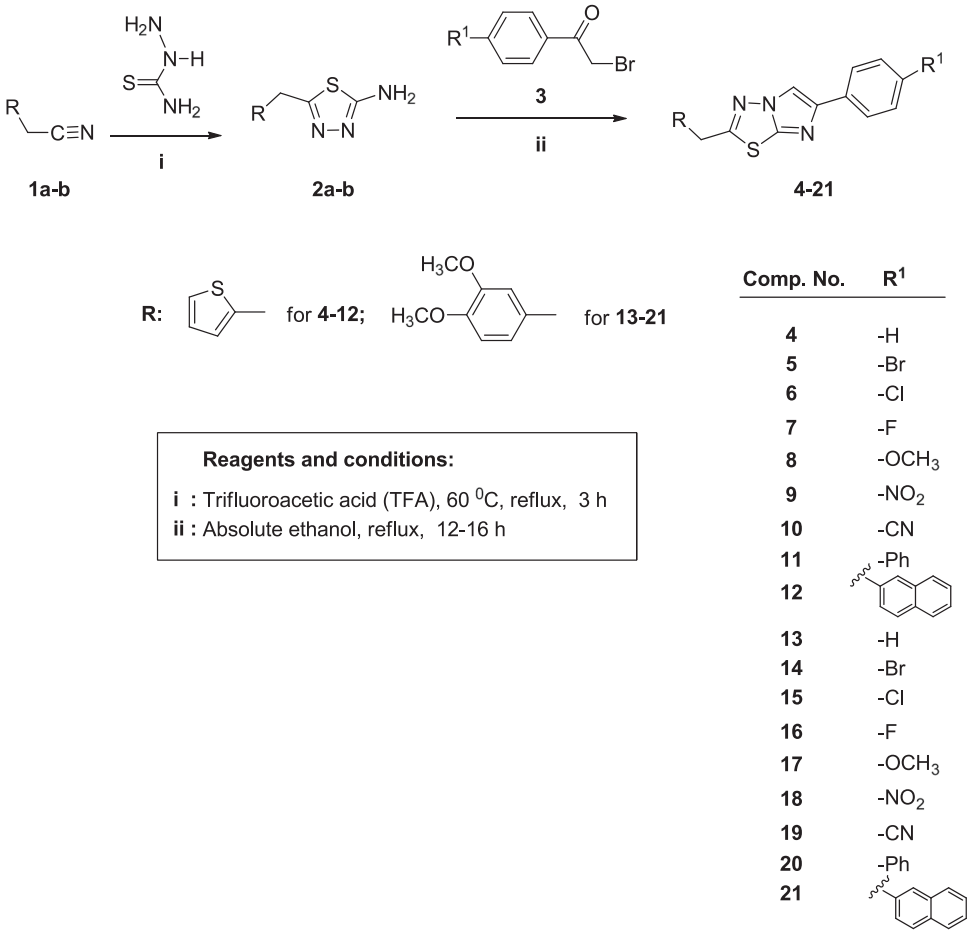

representing the C5-H signals in imidazo[2,1-*b*][1,3,4]thiadiazole derivatives **4–21**, which also provides distinct evidence for the formation of these compounds. This data is consistent with the literature (Lamani et al. 2009; Karki et al. 2011).

Signals that appeared in the 109.60–113.61 ppm range and the 143.17–145.68 ppm range in ^{13}C NMR spectra of these compounds are important evidence of ring cyclization. These signals correspond to the C5 and C6 carbons of imidazo[2,1-*b*][1,3,4]thiadiazole derivatives. Other ^{1}H NMR and ^{13}C NMR spectra data of these compounds are given in detail in the experimental part. The ^{1}H NMR and ^{13}C NMR spectra of all synthesized compounds are given in the Supplementary Material Section.

In addition, the mass spectra of all synthesized compounds were observed to be as expected and supported by molecular ion peaks.

The structures of compounds **7, 8, 10,** and **17** were also confirmed by X-ray diffraction analysis. The crystal structures and crystallographic data of compounds **7, 8, 10,** and **17** are shown in Fig. 1 and Table 1, respectively. In addition, rotational disorder was observed on the thiophene ring of the compound **10.** Bond lengths, bond angles and packing structures of compounds **7, 8, 10,** and **17** are given in the Supplementary Material Section.

Molecular docking studies

Molecular docking studies were performed to see possible binding modes of the synthesized compounds. A high resolution (1.6 Å) X-ray crystal structures of trichothecene 3-O-acetyltransferase (PDB ID: 2RKV) in complexed with Coenzyme A and T-2 mycotoxin (**ZBA**, native ligand) was used in calculations. Although it is well known that the docking software performs well in generating biologically active conformations of the ligands and identifying the binding modes to the target, however, the present scoring functions are not expected to discriminate between active and inactive compounds in such a success rate (Ece and Sevin 2013; Mascarenhasa and Ghoshal 2008). Docking scores of the compounds **4–21** together with that of the native ligand, **ZBA** are given in Table 2.

Glide docking performed well in ranking the most active compound **10** which has the second highest docking score amongst the synthesized compounds. **ZBA** has the highest docking score and it fits the binding pocket by making

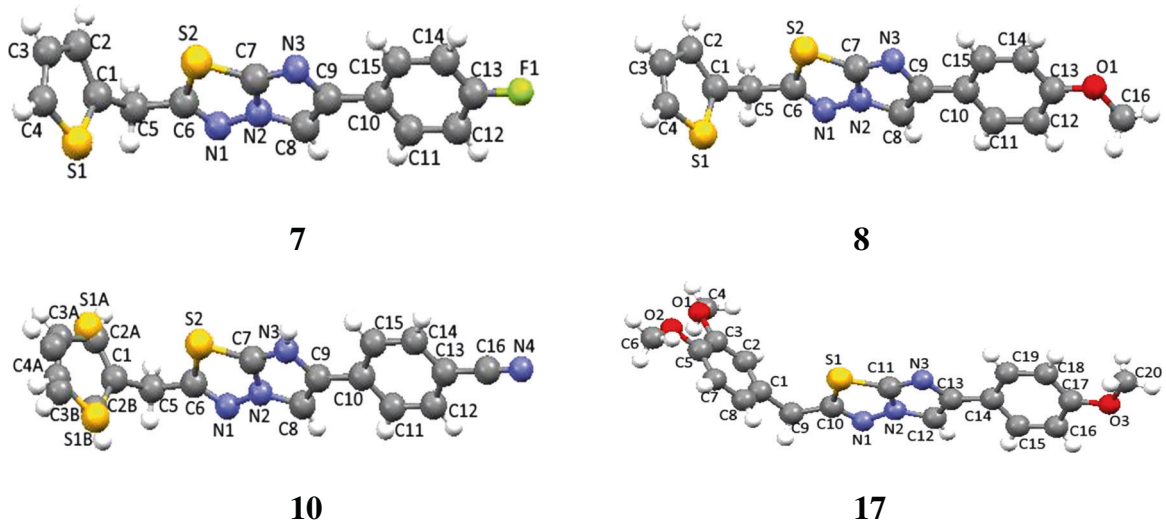

Fig. 1 The crystal structures of compounds **7**, **8**, **10,** and **17**

hydrogen bonds with Tyrosine 413 and Histidine 156 (Fig. 2). Although compound **10** does not make hydrogen bonds with the amino acid side chains of the target, it has a higher solvent exposure area that can in consequence, make the compound accommodate easily in the binding pocket without much conformational changes.

Binding surfaces of the target and **ZBA**, compounds **10** and **17** (the native ligand, the most and the least active compounds towards *Alternaria solani*, respectively) were generated and colored by electrostatic potential map (Fig. 3). *Red* color indicates high electron density regions while *blue* color shows low electron density zones. The binding conformation of compound **10** and **ZBA** look very similar. Compound **10** has favorable electrostatic interactions with the target. Low electron density region of the ligand interacts with the high electron density region in the active site. On the other hand, unfavorable interactions can be observed for the ligand **17**. Yet, its binding conformation is very different from **ZBA** and compound **10** (Fig. 3).

In vitro antifungal activity and SAR (structure-activity relationship) studies

Antifungal activity values (inhibition zone, percentage inhibition) of all synthesized compounds **(2a**, **2b,** and **4–21)** against plant pathogens are shown in Tables 3 and 4. All compounds used against plant pathogens showed varying levels of antifungal activity. Thiram 80% (reference drug) was used as a positive control. It showed 69% inhibition against *Alternaria solani*, 64% against *Fusarium oxysporum f. sp. Lycopersici*, and 43% against *Vertcillium dahliae*. Dimethylsulfoxide (DMSO), which was used as the negative control, showed no antifungal activity. Synthesized compounds were taken in four different doses (5, 2.5, 1.25 and 0.625 mg/mL) and showed 12–46% inhibition against *Alternaria solani*, 9–42% against *Fusarium oxysporum f. sp. Lycopersici*, and 2–32% against *Vertcillium dahliae*. Each compound showed varying levels of antifungal activity depending on the plant pathogens. The inhibition rates of compounds in the positive control demonstrate that the compounds produced moderate to high activities. We also calculated the LD_{50} values of the compounds (Fig. 4). According to these values, the most affected fungus type was *Alternaria solani*, followed by *Fusarium oxysporum f. sp. Lycopersici* and *Vertcillium dahliae*, respectively. LD_{50} dose values were in the 6.8–14.4 mg/mL range for *Alternaria solani*, in the 9.4–20.3 mg/mL range for *Fusarium oxysporum f. sp. Lycopersici*, and in the 8.6–43.3 mg/mL range for *Vertcillium dahliae*. Considering these inhibition rates and LD_{50} dose values, the highest antifungal activity was related to compounds **8**, **9**, **10**, **11**, and **16** for *Alternaria solani*; compounds **2a**, **6**, **10**, **11**, **13**, **15**, **19**, and **20** for *Fusarium oxysporum f. sp. Lycopersici*; and compounds **2b**, **6**, **10**, **11**, **12**, **13**, **16**, **19, 20**, and **21** for *Vertcillium dahliae*.

Furthermore, a structure-activity relationship (SAR) was also studied. Our primary aim in the SAR study was the modification of R group with thiophene and 3,4-dimethoxyphenyl moieties. Then, different substitution patterns were carefully selected as R^1 to confer the effect of different electronic environments on the activities. Thus, electron donating groups such as methoxy, phenyl and napthyl, and electron withdrawing groups such as nitro, cyano, fluoro, chloro, and bromo were chosen as substituents on structure of the target compounds (Fig. 5).

Table 1 Structural parameters of compounds **7, 8, 10,** and **17**

Compound No.	**7**	**8**	**10**	**17**
Molecular formula	$C_{15}H_{10}N_3FS_2$	$C_{16}H_{13}N_3OS_2$	$C_{16}H_{10}N_4S_2$	$C_{20}H_{19}N_3O_3S$
Molecular weight	315.38	327.41	322.41	381.44
Temperature (K)	293(2)	293(2)	293(2)	293(2)
Crystal system	Monoclinic	Monoclinic	Monoclinic	Triclinic
Space group	$P2_1$	$P2_1/n$	$P2_1$	P-1
a (Å)	10.4526(14)	13.9185(10)	10.8114(8)	5.7321(4)
b (Å)	5.5893(6)	5.5175(4)	5.6424(3)	11.6281(9)
c (Å)	12.5922(16)	21.0639(16)	12.8774(9)	14.8901(11)
α (°)	90	90	90	68.559(3)
β (°)	107.853(4)	107.981(2)	109.716(2)	81.069(3)
γ (°)	90	90	90	83.742(3)
Volume ($Å^3$)	700.24(15)	1538.6(2)	739.50(9)	911.12(12)
Z	2	4	2	2
ρ_{calc} (g/cm^3)	1.496	1.413	1.4524	1.390
μ (mm^{-1})	0.386	0.350	0.361	0.204
F(000)	324.0	680.0	334.6	400.0
Crystal size (mm^3)	0.17 × 0.15 × 0.13	0.27 × 0.22 × 0.18	0.2 × 0.17 × 0.15	0.2 × 0.18 × 0.15
Radiation	MoKα ($\lambda = 0.71073$)	MoKα ($\lambda = 0.71073$)	Mo Kα ($\lambda = 0.71073$)	MoKα ($\lambda = 0.71073$)
2Θ range for data collection (°)	6.07 to 49.992	5.924 to 56.732	6.04 to 56.58	7.056 to 50.998
Index ranges	$-13 \le h \le 13$, $-7 \le k \le 7$, $-16 \le l \le 16$	$-18 \le h \le 18$, $-7 \le k \le 7$, $-28 \le l \le 28$	$-14 \le h \le 14$, $-7 \le k \le 7$, $-15 \le l \le 17$	$-7 \le h \le 7$, $-15 \le k \le 15$, $-19 \le l \le 19$
Reflections collected	17,607	49,536	24,206	38,969
Independent reflections	2457 [$R_{int} = 0.0626$, $R_{sigma} = 0.0585$]	3819 [$R_{int} = 0.0379$, $R_{sigma} = 0.0197$]	3654 [$R_{int} = 0.0422$, $R_{sigma} = 0.0261$]	3362 [$R_{int} = 0.0790$, $R_{sigma} = 0.0403$]
Data/restraints/parameters	2457/1/191	3819/0/200	3654/8/212	3362/18/245
Goodness-of-fit on F^2	1.078	1.017	1.017	1.064
Final *R* indexes [$I>=2\sigma(I)$]	$R_1 = 0.0408$, $wR_2 = 0.0998$	$R_1 = 0.0610$, $wR_2 = 0.1457$	$R_1 = 0.0389$, $wR_2 = 0.0912$	$R_1 = 0.0564$, $wR_2 = 0.1452$
Final *R* indexes [all data]	$R_1 = 0.0612$, $wR_2 = 0.1123$	$R_1 = 0.0743$, $wR_2 = 0.1568$	$R_1 = 0.0631$, $wR_2 = 0.1064$	$R_1 = 0.0651$, $wR_2 = 0.1603$
Largest diff. peak/hole ($eÅ^{-3}$)	0.24/−0.27	0.50/−0.49	0.19/−0.34	0.57/−0.38
Flack parameter	0.06(3)		0.05(9)	
CCDC	1,448,275	1,448,280	1,448,274	1,448,273

In general, when *R* is the thiophene ring, the compounds **4–12** showed a higher activity (Tables 3 and 4, Fig. 4). Steric hindrance of 3,4-dimethoxyphenyl compared to thiophene could be attributed to this observation. As can be seen from Fig. 3, binding conformation of the least active compound **17** (towards *Alternaria solani*) is very different from that of the native ligand **ZBA** and the most active compound **10**. We believe that the bulky group forces compound **17** to fit into the binding pocket in a vertical position relative to **ZBA** and compound **10**.

In an attempt to see the substitution effect on the observed activities, we calculated highest occupied molecular orbital (HOMO) energy values and also octanol-water partition coefficients (QPlogPo/w) which shows the hydrophilic/hydrophobic property of the compounds studied. According to the QPlogPo/w values tabulated in Table 2, hydrophilic character is clearly one of the crucial factors that enhances activity. The active compounds also seem to have low HOMO energy values. Compound **10** which is found to be the highest active compound towards all three pathogens, has the lowest octanol-water partition coefficient. It also has one of the lowest HOMO energy value which results from the electron withdrawing substituent, –CN. The least active compound **17** towards

Table 2 Docking score and selected molecular properties of **ZBA** and the compounds **4–21**

Compound No.	DScore (kcal/mol)	E HOMO (eV)	QPlogPo/w
ZBA	−7.967	−10.23	2.084
4	−5.692	−8.81	4.646
5	−5.809	−8.95	5.230
6	−5.802	−8.77	5.150
7	−6.035	−8.91	4.884
8	−5.371	−8.54	4.710
9	−4.888	−9.48	3.895
10	−6.188	−9.11	3.804
11	−5.690	−8.51	6.315
12	−6.676	−8.40	7.309
13	−5.570	−8.81	4.844
14	−5.760	−8.95	5.428
15	−5.929	−8.76	5.349
16	−6.173	−8.90	5.083
17	−5.619	−8.53	4.911
18	−4.868	−9.47	4.097
19	−5.389	−9.11	4.002
20	−5.444	−8.52	6.511
21	−5.377	−8.39	7.493

Alternaria solani has high HOMO energy as can be expected from electron donating –OCH_3 group.

The combination of experimental findings on SAR study and computational works revealed that the presence of electron-withdrawing groups and less bulky groups at the para position on benzene ring have significant effects on the antifungal activity.

Conclusion

In conclusion, imidazo[2,1-*b*][1,3,4]thiadiazole derivatives, the target compounds of this study, were synthesized with simple and practical methods. The structures of synthesized compounds were elucidated by various spectroscopic methods, including IR, ^{1}H NMR, ^{13}C NMR, elemental analysis, mass spectroscopy and X-ray diffraction analysis. The in vitro antifungal activity of the synthesized compounds was evaluated against plant pathogens. Most of the compounds showed considerable antifungal activity. In addition, molecular docking studies were performed for all synthesized compounds to determine the potential binding mode of inhibitors. From the SAR study and with the help of computational works, it was observed that the presence of electron-withdrawing and low steric groups at the para position on benzene ring enhanced the antifungal activity. The best active compound **10** was found to have the lowest octanol/water partition coefficient, high HOMO energy and high docking score.

The molecular docking results, along with the biological assay data, show that all the synthesized compounds have promising biological activities and might be novel potential drug candidates.

Experimental section

General methods

The ^{1}H NMR and ^{13}C NMR spectra of the compounds were measured in DMSO-d_6 using an Agilent NMR VNMRS spectrometer at 400 MHz and 100 MHz, respectively. Chemical shift values are given in ppm (δ) with tetramethylsilane as the internal standard. The IR spectra were recorded in a Bruker Optics Alpha Fourier transform-infrared in attenuated total reflectance (ATR). The mass spectra were measured with a Thermo TSQ Quantum Access Max LC-MS/MS spectrometer. Elemental analyses were performed for a LECO 932 CHNS (Leco-932, St. Joseph, MI, USA) instrument and the results were within ± 0.4% of the theoretical values. Melting points were recorded on a Thermo Scientific IA9000 series apparatus and were uncorrected. The nitrile derivatives **(1a–b)** were procured from commercial suppliers (Biostar-Turkey). All the chemicals, reagents and solvents were directly purchased from Sigma-Aldrich (St. Louis, MO) and were used without further purification, unless mentioned specifically.

Crystallographic analysis

A suitable crystal was selected and placed (Bruker 2008) on a 'Bruker APEX-II CCD' diffractometer. The crystal was kept at 293(2) K during the data collection process. Using Olex2 (Dolomanov et al. 2009), the structure was determined by the ShelXT (Sheldrick 2015) structure solution program using Direct Methods and refined with the ShelXL (Sheldrick 2015) refinement package using Least Squares minimization. The positions of hydrogen atoms were obtained geometrically according to the overlap method. When placing hydrogen atoms geometrically, the bond length was fixed as aromatic C–H 0.93 Å, methylene C-H_2 at 0.97 Å, and methyl C–H_3 at 0.96 Å.

Fungal isolate

The following plant pathogens were used in the antifungal activity studies: *Alternaria solani*, *Fusarium oxysporum f. sp. lycopersici* and *Vertcillium dahliae*. The fungal pathogens were isolated from tomatoes in Antalya, Turkey.

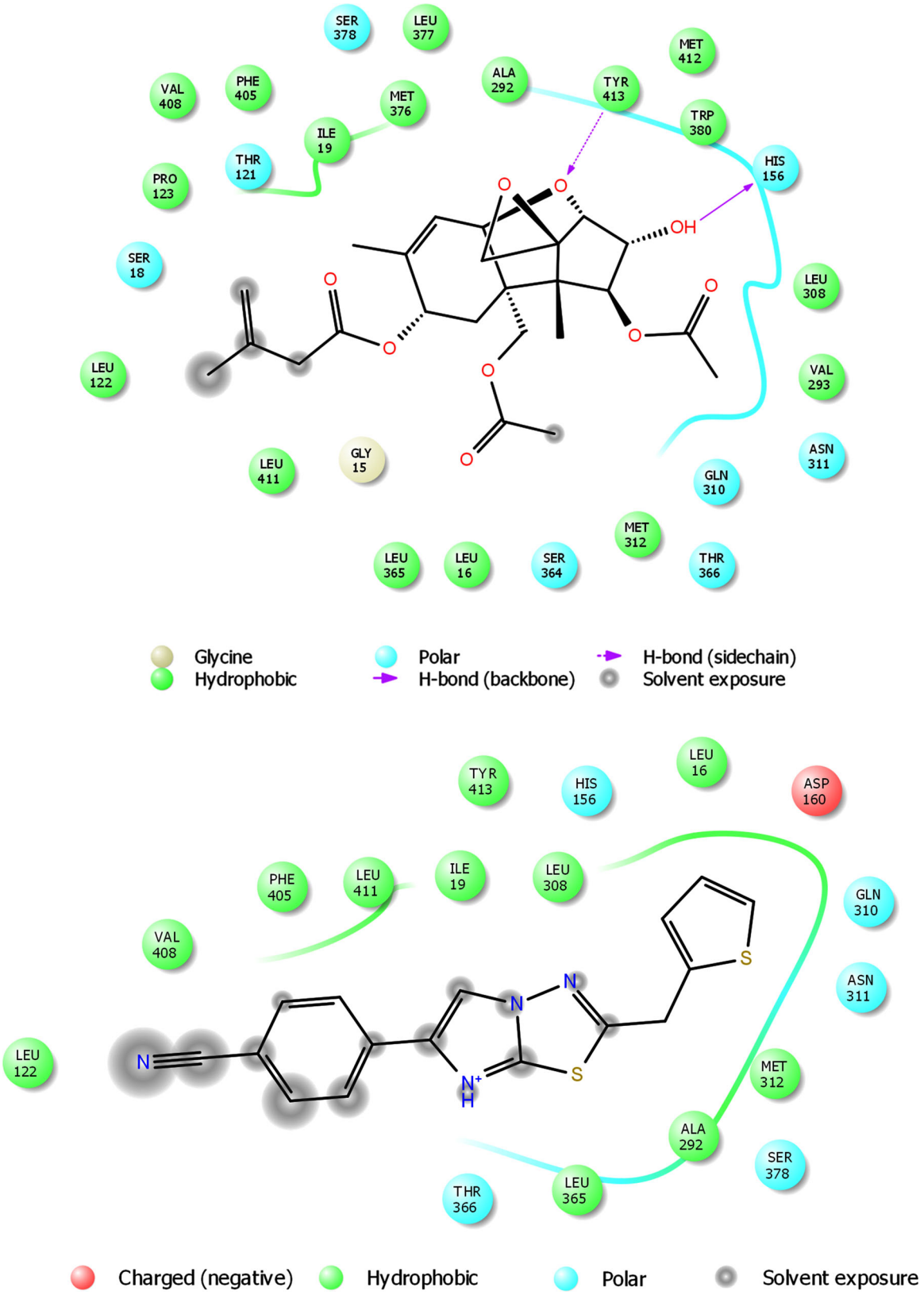

Fig. 2 2D ligand interaction diagram for ZBA (*top*) and compound **10** (*bottom*)

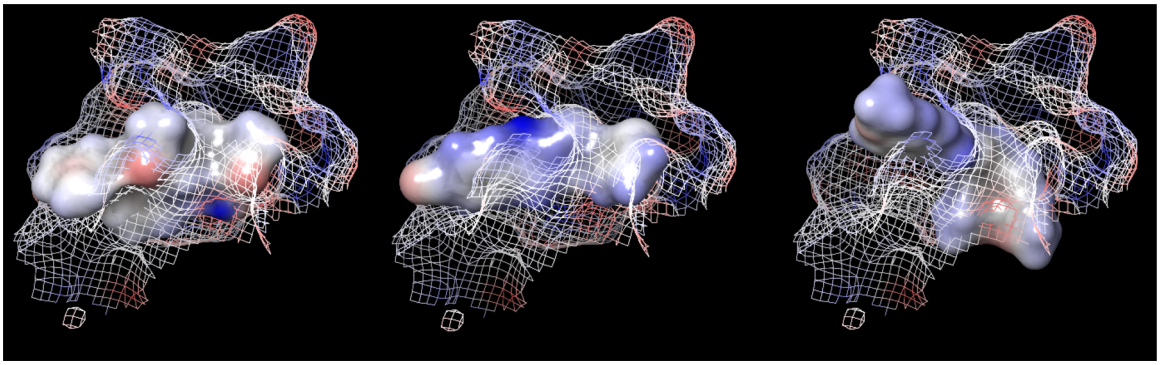

Fig. 3 Binding surface of the target together with **ZBA** (*left*), compound **10** (*middle*) and compound **17** (right)

The pathogens were grown on a PDA (potato dextrose agar) medium at 22 ± 2 °C for about 7 days.

Computational section

Ligand and protein preparation

Before going any further in computational works, all the compounds have to be prepared for calculations. Hence, the compounds **4–21** were prepared using LigPrep module of Schrödinger suite. Optimized potential liquid simulations 3 (OPLS3) force field was used for minimizations (Harder et al. 2015). All possible states of the compounds at pH 7.0 ± 2.0 were generated.

Molecular docking studies were carried out using X-ray crystal structures of trichothecene 3-O-acetyltransferase (PDB ID: 2RKV) in complexed with Coenzyme A and T-2 mycotoxin (**ZBA**) having a resolution of 1.6 Å. Prior to calculations, this raw crystal structure was prepared using the Protein Preparation Wizard (PrepWizard) in Maestro of Schrödinger software package (Schrödinger 2016a). As a first step, hydrogen atoms were added and any water and heteroatoms except native ligand (**ZBA**) were removed in the PrepWizard. The protein structure was then refined by correcting the missing side chain atoms and assigning the bond orders. After the optimization step, in order to remove the steric clashes between the atoms, the refined structure was further minimized using OPLS3 force field.

Molecular docking

The docking calculations were performed using the Glide SP (standard precision) module of Schrödinger Suite (Friesner et al. 2004; Halgren et al. 2004; Friesner et al. 2006). A grid that represents the binding pocket was generated using the default settings. The native ligand was used as a reference to choose the center and size of the receptor grid.

Calculation of molecular properties

HOMO enery values were calculated using Wavefunction's Spartan '16 parallel suite (Spartan 16, Wavefunction Inc., Irvine CA). The equilibrium geometry and orbital energies of each compound were calculated at ground state using Semi-Empirical Parametric model number 3 (PM3). QikProp module of Schrodinger was used to calculate octanol-water partition coefficients of the compounds (Schrödinger 2016b).

Synthesis

*General procedure for the synthesis of imidazo[2,1-*b*][1,3,4]thiadiazole derivatives* ***4–21***

In a two-necked flask, 2-amino-1,3,4-thiadiazole derivatives **2a–b** (0.004 mol) were dissolved in absolute ethanol (30 mL). Phenacyl bromide derivatives **3a–i** (0.04 mol) were also dissolved in absolute ethanol (20 mL) and then added drop by drop to this solution at room temperature with the assistance of a dropping funnel. The mixture was then refluxed and stirred for 12–16 h. The progress of reaction was monitored by thin layer chromatographyat appropriate time intervals. The excess solvent was removed under reduced pressure and neutralized by an aqueous sodium carbonate (Na_2CO_3) solution. The solution was filtered and washed with deionized water. The solid matter was recrystallized from acetone. The synthesized compounds were dried with P_2O_5 in a vacuum oven. The physical properties and spectral data derived from the obtained products are listed below.

Table 3 Antifungal activity (inhibition zone) of all compounds against plant pathogens

Compound No.	*Alternaria solani*				*F. oxysporum f. sp. Lycopersici*				*Verticillium dahliae*			
	Doses (mg/mL)				Doses (mg/mL)				Doses (mg/mL)			
	5	2.5	1.25	0.625	5	2.5	1.25	0.625	5	2.5	1.25	0.625
2a	*10.8 ± 0.3	9.5 ± 0.4	7.3 ± 0.3	6.1 ± 0.3	10.9 ± 0.4	8.5 ± 0.5	6.5 ± 0.1	3.6 ± 0.2	6.4 ± 0.5	3.8 ± 0.2	2.1 ± 0.3	0.7 ± 0.1
2b	11.4 ± 0.3	8.2 ± 0.1	5.7 ± 0.5	5.1 ± 0.7	9.7 ± 0.4	9.0 ± 0.4	7.0 ± 0.1	3.5 ± 0.4	7.7 ± 0.8	4.3 ± 0.6	2.0 ± 0.4	0.8 ± 0.1
4	9.4 ± 0.3	7.5 ± 0.3	6.0 ± 0.2	5.1 ± 0.3	9.6 ± 0.9	7.9 ± 0.5	6.8 ± 0.2	2.8 ± 0.2	6.3 ± 0.8	3.9 ± 0.1	2.0 ± 0.1	0.9 ± 0.1
5	9.9 ± 0.4	7.7 ± 0.2	5.5 ± 0.4	3.9 ± 0.2	9.3 ± 0.7	8.2 ± 0.3	6.4 ± 0.1	3.4 ± 0.4	5.9 ± 0.3	3.9 ± 0.4	2.5 ± 0.3	1.8 ± 0.1
6	10.8 ± 0.3	6.8 ± 0.2	4.9 ± 0.2	4.5 ± 0.3	11.8 ± 0.2	9.3 ± 0.6	6.6 ± 0.3	3.9 ± 0.2	8.1 ± 1.1	5.9 ± 0.9	4.5 ± 0.2	1.4 ± 0.2
7	10.3 ± 0.3	8.3 ± 0.4	6.4 ± 0.7	5.4 ± 0.3	10.5 ± 0.6	7.9 ± 0.2	6.7 ± 0.3	4.4 ± 0.3	6.9 ± 0.4	3.7 ± 0.2	2.0 ± 0.2	0.8 ± 0.1
8	11.6 ± 0.7	9.1 ± 0.1	6.7 ± 0.6	4.8 ± 0.1	10.5 ± 0.6	8.3 ± 0.5	6.3 ± 0.3	2.8 ± 0.2	7.0 ± 0.2	4.0 ± 0.3	3.4 ± 0.2	1.4 ± 0.2
9	13.1 ± 0.6	10.7 ± 02	8.9 ± 0.4	6.8 ± 0.3	9.6 ± 0.6	8.9 ± 0.4	7.9 ± 0.3	4.5 ± 0.3	6.2 ± 0.0	3.9 ± 0.3	2.4 ± 0.3	0.5 ± 0.2
10	13.2 ± 0.5	9.6 ± 0.4	7.9 ± 0.1	6.9 ± 0.2	11.7 ± 0.4	7.9 ± 0.1	6.8 ± 0.2	3.2 ± 0.2	9.7 ± 0.5	6.3 ± 0.2	2.1 ± 0.1	0.7 ± 0.3
11	11.7 ± 0.4	8.6 ± 0.3	6.8 ± 0.2	5.1 ± 0.4	11.1 ± 1.0	8.0 ± 0.9	5.9 ± 0.2	3.3 ± 0.4	8.7 ± 0.4	5.1 ± 0.2	3.5 ± 0.2	1.3 ± 0.2
12	10.5 ± 0.4	8.8 ± 0.1	5.2 ± 0.3	4.2 ± 0.3	10.0 ± 0.2	7.6 ± 0.3	5.5 ± 0.3	3.3 ± 0.5	7.5 ± 0.7	4.7 ± 0.7	3.4 ± 0.3	1.4 ± 0.2
13	9.9 ± 0.2	8.9 ± 0.4	6.8 ± 0.2	4.0 ± 0.2	10.6 ± 0.1	6.7 ± 0.3	5.6 ± 0.3	3.1 ± 0.2	8.3 ± 0.5	5.9 ± 0.2	3.6 ± 0.2	1.4 ± 0.3
14	8.7 ± 0.4	6.7 ± 0.2	4.7 ± 0.3	3.6 ± 0.4	9.8 ± 0.3	7.8 ± 0.4	6.1 ± 0.4	3.4 ± 0.3	6.5 ± 0.8	4.6 ± 0.1	2.4 ± 0.3	1.3 ± 0.2
15	10 ± 0.3	6.7 ± 0.1	5.4 ± 0.2	4.9 ± 0.3	10.7 ± 0.2	7.5 ± 0.5	5.6 ± 0.1	3.6 ± 0.2	6.9 ± 1.0	4.1 ± 0.2	2.7 ± 0.1	0.7 ± 0.1
16	11.6 ± 0.4	7.6 ± 0.4	5.8 ± 0.1	4.4 ± 0.2	9.3 ± 0.3	7.7 ± 0.2	6.3 ± 0.1	3.3 ± 0.4	8.5 ± 0.3	5.6 ± 0.1	4.3 ± 0.2	1.4 ± 0.2
17	8.2 ± 0.3	6.6 ± 0.3	5.0 ± 0.3	4.3 ± 0.3	10.0 ± 0.3	7.7 ± 0.3	5.1 ± 0.2	3.0 ± 0.4	7.2 ± 0.3	4.7 ± 0.5	1.6 ± 0.3	0.8 ± 0.3
18	10.7 ± 0.4	6.9 ± 0.4	5.4 ± 0.2	4.6 ± 0.3	9.0 ± 0.3	6.1 ± 0.1	5.7 ± 0.1	3.4 ± 0.2	6.4 ± 0.8	4.3 ± 0.2	2.9 ± 0.2	1.8 ± 0.3
19	10.6 ± 0.2	9.5 ± 0.2	7.4 ± 0.4	5.2 ± 0.2	10.8 ± 0.5	7.4 ± 0.4	6.0 ± 0.7	3.2 ± 0.3	8.2 ± 0.8	5.1 ± 0.3	2.6 ± 0.2	1.0 ± 0.0
20	10.6 ± 0.2	8.6 ± 0.1	7.6 ± 0.2	5.6 ± 0.3	10.9 ± 0.4	7.0 ± 0.5	5.1 ± 0.1	2.7 ± 0.7	7.8 ± 0.3	4.4 ± 0.3	3.3 ± 0.2	1.2 ± 0.2
21	9.6 ± 0.2	8.5 ± 1.0	7.0 ± 0.2	4.4 ± 0.3	10.3 ± 0.6	7.3 ± 0.4	5.0 ± 0.1	2.8 ± 0.1	7.4 ± 0.2	3.8 ± 0.2	2.4 ± 0.3	1.3 ± 0.2
C+	19.89 ± 0.6				19.25 ± 0.1				12.90 ± 0.1			
C−	0.97 ± 0.1				1.79 ± 0.5				0.00 ± 0.0			

C+ (Thiram 80%): Positive control; C− (DMSO): Negative Control

*Inhibition zone ± standard deviation

Table 4 Percentage inhibition of all new compounds against plant pathogens

Compound No.	*Alternaria solani*				*F. oxysporum f. sp. lycopersici*				*Verticillium dahliae*			
	Doses (mg/mL)				Doses (mg/mL)				Doses (mg/mL)			
	5	2.5	1.25	0.625	5	2.5	1.25	0.625	5	2.5	1.25	0.625
2a	37	33	25	21	39	30	23	13	21	13	7	2
2b	39	28	19	18	34	32	25	12	26	14	7	3
4	32	26	21	18	34	28	24	10	21	13	7	3
5	34	26	19	13	33	29	23	12	20	13	8	6
6	37	23	17	16	42	33	23	14	27	20	15	5
7	35	29	22	19	37	28	24	16	23	12	7	3
8	40	31	23	16	37	29	22	10	23	13	11	5
9	45	37	31	24	34	32	28	16	21	13	8	2
10	46	33	27	24	41	28	24	11	32	21	7	2
11	40	30	23	18	39	29	21	12	29	17	12	4
12	36	30	18	14	35	27	20	12	25	16	11	5
13	34	31	23	14	38	24	20	11	28	20	12	5
14	30	23	16	12	35	28	22	12	22	15	8	4
15	34	23	19	17	38	27	20	13	23	14	9	2
16	40	26	20	15	33	27	22	12	28	19	14	5
17	28	23	17	15	35	27	18	11	24	16	5	3
18	37	24	19	16	32	22	20	12	21	14	10	6
19	37	33	26	18	38	26	21	11	27	17	9	3
20	36	30	26	19	39	25	18	9	26	15	11	4
21	33	29	24	15	37	26	18	10	25	13	8	4
C+	69%				64%				43%			
C−	3% *(29,03 mm)				6% *(28,21mm)*				0% *(30,00 mm)			

C+ (Thiram 80%): Positive control; C− (DMSO): Negative Control

* According to negative control, mycelial growth was calculated by percentage inhibition values.

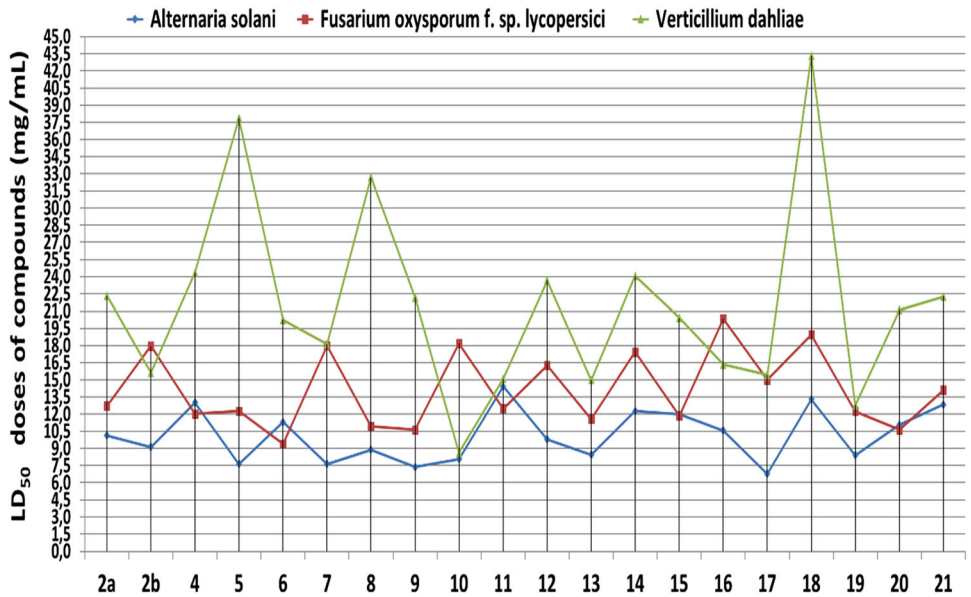

Fig. 4 LD_{50} doses of all compounds against plant pathogens. LD_{50} values were calculated from dose-response by Probit analysis

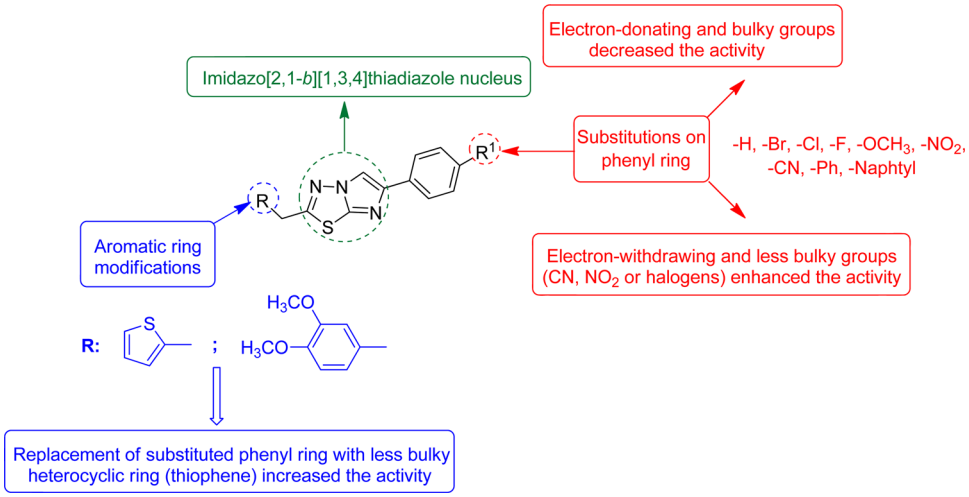

Fig. 5 SAR of imidazo[2,1-*b*][1,3,4]thiadiazole derivatives as antifungal agents

*6-Phenyl-2-(thiophen-2-ylmethyl)imidazo[2,1-b][1,3,4]thiadiazole (**4**)*

Light yellow crystals, yield 0.74 g (62%), mp 167–169 °C (from Acetone); IR (ATR, cm^{-1}): 3110 (Ar–CH), 2979 (Aliph. CH), 1594 (C=N); ^{1}H NMR (400 MHz, DMSO-d_6, δ ppm): 4.68 (s, 2H, -CH_2), Thiophene-H [7.02 (t, $J = 8.0$ Hz, 1H), 7.13 (d, $J = 4.0$ Hz, 1H), 7.49 (d, $J = 4.0$ Hz, 1H)], Phenyl-H [7.25 (t, $J = 12.0$ Hz, 1H), 7.38 (t, $J = 12.0$, 2H), 7.83 (d, $J = 8.0$ Hz, 2H)], Imidazole-H [8.64 (s, 1H)]; ^{13}C NMR (100 MHz, DMSO-d_6, δ ppm): 31.65 (–CH_2), Thiophene-C [125.08 (CH), 126.80 (CH), 127.72 (CH), 145.41 (C)], Phenyl-C [127.82 (CH), 128.09 (CH), 129.10 (CH), 134.30 (C)], Imidazole-C [110.77 (CH), 145.32 (C)], Thiadiazole-C [137.83 (C), 164.43 (C)]; MS: *m/z* 298.18 (M +1, 100). Anal. Calcd. for $C_{15}H_{11}N_3S_2$: C, 60.58; H, 3.73; N, 14.13. Found: C, 60.64; H, 3.79; N, 14.16.

*6-(4-Bromophenyl)-2-(thiophen-2-ylmethyl)imidazo[2,1-b][1,3,4]thiadiazole (**5**)*

Light gray crystals, yield 0.89 g (59%), mp 176–178 °C (from Acetone); IR (ATR, cm^{-1}): 3128 (Ar–CH), 2981 (Aliph. CH), 1596 (C=N); ^{1}H NMR (400 MHz, DMSO-d_6, δ ppm): 4.68 (s, 2H, –CH_2), Thiophene-H [7.02 (t, $J = 8.0$ Hz, 1H), 7.13 (d, $J = 4.0$ Hz, 1H), 7.49 (d, $J = 4.0$ Hz, 1H)], Phenyl-H [7.57 (dd, $J = 4.0$, 2.0 Hz, 2H), 7.78 (dd, $J = 4.0$, 2.0 Hz, 2H)], Imidazole-H [8.70 (s, 1H)]; ^{13}C NMR (100 MHz, DMSO-d_6, δ ppm): 31.65 (–CH_2), Thiophene-C [126.83 (CH), 127.06 (CH), 127.82 (CH), 145.56 (C)], Phenyl-C [120.59 (C), 128.10 (CH), 132.03 (C), 133.59 (CH)], Imidazole-C [111.24 (CH), 144.23 (C)], Thiadiazole-C [137.76 (C), 164.77 (C)]; MS: *m/z* 376.19 (M^+, 95), 378.15 (M+2, 100). Anal. Calcd. for $C_{15}H_{10}BrN_3S_2$: C, 47.88; H, 2.68; N, 11.17. Found: C, 47.84; H, 2.65; N, 11.14.

*6-(4-Chlorophenyl)-2-(thiophen-2-ylmethyl)imidazo[2,1-b][1,3,4]thiadiazole (**6**)*

Gray crystals, yield 70.81 g (61%), mp 170–172 °C (from Acetone); IR (ATR, cm^{-1}): 3124 (Ar–CH), 2974 (Aliph. CH), 1594 (C=N); ^{1}H NMR (400 MHz, DMSO-d_6, δ ppm): 4.68 (s, 2H, –CH_2), Thiophene-H [7.02 (t, $J = 8.0$ Hz, 1H), 7.13 (d, $J = 4.0$ Hz, 1H), 7.49 (d, $J = 4.0$ Hz, 1H)], Phenyl-H [7.43 (dd, $J = 3.6$, 2.0 Hz, 2H), 7.84 (dd, $J = 3.6$, 2.0 Hz, 2H)], Imidazole-H [8.68 (s, 1H)]; ^{13}C NMR (100 MHz, DMSO-d_6, δ ppm): 31.64 (–CH_2), Thiophene-C [126.73 (CH), 126.82 (CH), 127.82 (CH), 145.54 (C)], Phenyl-C [128.11 (CH), 129.13 (CH), 132.07 (C), 133.22 (C)], Imidazole-C [111.20 (CH), 144.20 (C)], Thiadiazole-C [137.76 (C), 164.73 (C)]; MS: *m/z* 332.30 (M+1, 100). Anal. Calcd. for $C_{15}H_{10}ClN_3S_2$: C, 54.29; H, 3.04; N, 12.66. Found: C, 54.34; H, 3.00; N, 12.63.

*6-(4-Fluorophenyl)-2-(thiophen-2-ylmethyl)imidazo[2,1-b][1,3,4]thiadiazole (**7**)*

Light yellowish crystals, yield 0.81 g (64%), mp 172–173 °C (from Acetone); IR (ATR, cm^{-1}): 3139 (Ar–CH), 2941 (Aliph. CH), 1585 (C=N); ^{1}H NMR (400 MHz, DMSO-d_6, δ ppm): 4.68 (s, 2H, –CH_2), Thiophene-H [7.02 (q, $J = 8.0$ Hz, 1H), 7.13 (d, $J = 4.0$ Hz, 1H), 7.48 (t, $J = 8.0$ Hz, 1H)], Phenyl-H [7.22 (t, $J = 12.0$ Hz, 2H), 7.86 (q, $J = 12.0$, 2H)], Imidazole-H [8.62 (s, 1H)]; ^{13}C NMR (100 MHz, DMSO-d_6, δ ppm): 31.63 (–CH_2), Thiophene-C [126.80 (CH), 127.04 (CH), 127.81 (CH), 145.36 (C)], Phenyl-C [116.08 (CH), 128.09 (CH), 130.87 (C), 163.16 (C)], Imidazole-C [110.62 (CH), 144.50 (C)], Thiadiazole-C

[137.80 (C), 164.46 (C)]; MS: *m/z* 315.96 (M^+, 100). Anal. Calcd. for $C_{15}H_{10}FN_3S_2$: C, 57.12; H, 3.20; N, 13.32. Found: C, 57.22; H, 3.25; N, 13.35.

*6-(4-Methoxyphenyl)-2-(thiophen-2-ylmethyl)imidazo[2,1-b][1,3,4]thiadiazole (**8**)*

Light yellow crystals, yield 0.84 g (64%), mp 166–167 °C (from Acetone); IR (ATR, cm^{-1}): 3127 (Ar–CH), 2923 (Aliph. CH), 1599 (C=N); ^{1}H NMR (400 MHz, DMSO-d_6, δ ppm): 3.76 (s, 3H, –OCH_3), 4.67 (s, 2H, –CH_2), Thiophene-H [7.02 (t, $J = 8.0$ Hz, 1H), 7.13 (d, $J = 4.0$ Hz, 1H), 7.49 (d, $J = 4.0$ Hz, 1H)], Phenyl-H [6.95 (d, $J = 8.0$ Hz, 2H), 7.75 (d, $J = 8.0$, 2H)], Imidazole-H [8.51 (s, 1H)]; ^{13}C NMR (100 MHz, DMSO-d_6, δ ppm): 31.63 (–CH_2), 55.56 (-OCH_3), Thiophene-C [126.78 (CH), 126.98 (CH), 127.80 (CH), 145.48 (C)], Phenyl-C [114.52 (CH), 126.42 (C), 128.04 (CH), 159.12 (C)], Imidazole-C [109.60 (CH), 145.03 (C)], Thiadiazole-C [137.89 (C), 163.92 (C)]; MS: *m/z* 328.19 (M+1, 100). Anal. Calcd. for $C_{16}H_{13}N_3OS_2$: C, 58.69; H, 4.00; N, 12.83. Found: C, 58.64; H, 4.04; N, 12.88.

*6-(4-Nitrophenyl)-2-(thiophen-2-ylmethyl)imidazo[2,1-b][1,3,4]thiadiazole (**9**)*

Yellow solid, yield 0.81 g (59%), mp 216–218 °C (from Acetone); IR (ATR, cm^{-1}): 3125 (Ar–CH), 2947 (Aliph. CH), 1597 (C=N), 1520, 1336 (NO_2); ^{1}H NMR (400 MHz, DMSO-d_6, δ ppm): 4.71 (s, 2H, -CH_2), Thiophene-H [7.03 (s, 1H), 7.14 (s, 1H), 7.50 (d, $J = 4.0$ Hz, 1H)], Phenyl-H [8.09 (d, $J = 8.0$ Hz, 2H), 8.26 (d, $J = 8.0$, 2H], Imidazole-H [8.94 (s, 1H)]; ^{13}C NMR (100 MHz, DMSO-d_6, δ ppm): 31.67 (–CH_2), Thiophene-C [126.90 (CH), 127.84 (CH), 128.20 (CH), 145.89 (C)], Phenyl-C [124.67 (CH), 125.70 (CH), 140.86 (C), 146.55 (C)], Imidazole-C [113.53 (CH), 143.17 (C)], Thiadiazole-C [137.60 (C), 165.77 (C)]; MS: *m/z* 343.22 (M+1, 100). Anal. Calcd. for $C_{15}H_{10}N_4O_2S_2$: C, 52.62; H, 2.94; N, 16.36. Found: C, 52.65; H, 2.98; N, 16.31.

*4-(2-(Thiophen-2-ylmethyl)imidazo[2,1-b][1,3,4]thiadiazol-6-yl)benzonitrile (**10**)*

Gray crystals, yield 0.62 g (52%), mp 210–212 °C (from Acetone); IR (ATR, cm^{-1}): 3109 (Ar–CH), 2930 (Aliph. CH), 2277 (C≡N), 1589 (C=N); ^{1}H NMR (400 MHz, DMSO-d_6, δ ppm): 4.70 (s, 2H, -CH_2), Thiophene-H [7.03 (t, $J = 8.0$ Hz, 1H), 7.13 (d, $J = 4.0$ Hz, 1H), 7.49 (d, $J = 4.0$ Hz, 1H)], Phenyl-H [7.85 (dd, $J = 4.0$, 2.0 Hz, 2H), 8.01 (dd, $J = 4.0$, 2.0 Hz, 2H], Imidazole-H [8.87 (s, 1H)]; ^{13}C NMR (100 MHz, DMSO-d_6, δ ppm): 31.66 (-CH_2), 119.48 (C≡N), Thiophene-C [126.87 (CH), 127.83 (CH), 128.18 (CH), 146.17 (C)], Phenyl-C [112.95 (C), 125.54 (CH), 133.21 (CH), 138.82 (C)], Imidazole-C [109.75 (CH), 143.55 (C)], Thiadiazole-C [137.64 (C), 165.50 (C)]; MS: *m/z* 322.82 (M^+, 100). Anal. Calcd. for $C_{16}H_{10}N_4S_2$: C, 59.61; H, 3.13; N, 17.38. Found: C, 59.58; H, 3.18; N, 17.35.

*6-([1,1′-Biphenyl]-4-yl)-2-(thiophen-2-ylmethyl)imidazo[2,1-b][1,3,4]thiadiazole (**11**)*

Gray solid, yield 0.97 g (65%), mp 190–191 °C (from Acetone); IR (ATR, cm^{-1}): 3093 (Ar–CH), 2961 (Aliph. CH), 1580 (C=N); ^{1}H NMR (400 MHz, DMSO-d_6, δ ppm): 4.69 (s, 2H, –CH_2), Thiophene-H [7.02 (s, 1H), 7.13 (s, 1H), 7.50 (s, 1H)], Phenyl-H [7.69 (d, $J = 8.0$ Hz, 2H), 7.92 (d, $J = 8.0$, 2H)], Phenyl-Phenyl-H [7.35 (t, $J = 8.0$ Hz, 1H), 7.45–7.43 (m, 4H)], Imidazole-H [8.70 (s, 1H)]; ^{13}C NMR (100 MHz, DMSO-d_6, δ ppm): 31.65 (–CH_2), Thiophene-C [125.62 (CH), 126.82 (CH), 128.09 (CH), 145.45 (C)], Phenyl-C [127.82 (CH), 129.62 (CH), 133.46 (C), 140.16 (C)], Phenyl-Phenyl-C [126.90 (CH), 127.54 (CH), 129.39 (CH), 139.31 (C)], Imidazole-C [110.96 (CH), 145.06 (C)], Thiadiazole-C [137.84 (C), 164.50 (C)]; MS: *m/z* 373.85 (M^+, 100). Anal. Calcd. for $C_{21}H_{15}N_3S_2$: C, 67.53; H, 4.05; N, 11.25. Found: C, 67.60; H, 4.09; N, 11.29.

*6-(Naphthalen-2-yl)-2-(thiophen-2-ylmethyl)imidazo[2,1-b][1,3,4]thiadiazole (**12**)*

Gray solid, yield 0.76 g (55%), mp 170–172 °C (from Acetone); IR (ATR, cm^{-1}): 3109 (Ar–CH), 2942 (Aliph. CH), 1584 (C=N); ^{1}H NMR (400 MHz, DMSO-d_6, δ ppm): 4.70 (s, 2H, –CH_2), Thiophene-H [7.03 (t, $J = 8.0$ Hz, 1H), 7.14 (d, $J = 4.0$ Hz, 1H), 7.49 (d, $J = 4.0$ Hz, 1H)], Naphthyl-H [7.50–7.47 (m, 2H), 7.93–7.87 (m, 3H), 7.99 (d, $J = 8.0$ Hz, 1H), 8.38 (s, 1H)], Imidazole-H [8.77 (s, 1H)]; ^{13}C NMR (100 MHz, DMSO-d_6, δ ppm): 31.67 (-CH_2), Thiophene-C [126.84 (CH), 127.84 (CH), 128.62 (CH), 145.61 (C)], Naphtyl-C [123.18 (CH), 123.86 (CH), 126.24 (CH), 128.08 (CH), 128.13 (CH), 128.37 (CH), 131.79 (C), 132.82 (C), 133.68 (C)], Imidazole-C [111.33 (CH), 145.38 (C)], Thiadiazole-C [137.81 (C), 164.56 (C)]; MS: *m/z* 347.95 (M^+, 100). Anal. Calcd. for $C_{19}H_{13}N_3S_2$: C, 65.68; H, 3.77; N, 12.09. Found: C, 65.65; H, 3.81; N, 12.14.

*2-(3,4-Dimethoxybenzyl)-6-phenylimidazo[2,1-b][1,3,4]thiadiazole (**13**)*

White solid, yield 0.94 g (67%), mp 170–171 °C (from Acetone); IR (ATR, cm^{-1}): 3125 (Ar–CH), 2923 (Aliph. CH),

1591 (C=N); ^{1}H NMR (400 MHz, DMSO-d_6, δ ppm): 3.73 (s, 6H, 2-OCH_3), 4.33 (s, 2H, -CH_2), $(OCH_3)_2$Ar–H [6.93 (q, $J = 12.0$ Hz, 2H), 6.99 (s, 1H)], Phenyl-H [7.24 (t, $J = 12.0$ Hz, 1H), 7.38 (t, $J = 12.0$ Hz, 2H), 7.83 (d, $J = 8.0$ Hz, 2H)], Imidazole-H [8.61 (s, 1H)]; ^{13}C NMR (100 MHz, DMSO-d_6, δ ppm): 37.01 (–CH_2), 55.96 (–OCH_3), $(OCH_3)_2$Ar–C [110.67 (CH), 112.48 (CH), 121.74 (CH), 129.08 (C), 148.68 (C), 149.36 (C)], Phenyl-C [125.05 (CH), 127.66 (CH), 128.57 (CH), 134.36 (C)], Imidazole-C [113.31 (CH), 145.38 (C)], Thiadiazole-C [145.25 (C), 165.75 (C)]; MS: *m/z* 352.26 (M+1, 100). Anal. Calcd. for $C_{19}H_{17}N_3O_2S$: C, 64.94; H, 4.88; N, 11.96. Found: C, 64.99; H, 4.85; N, 11.92.

*6-(4-Bromophenyl)-2-(3,4-dimethoxybenzyl)imidazo[2,1-*b*][1,3,4]thiadiazole (**14**)*

Yellow solid, yield 1.19 g (69%), mp 172–174 °C (from Acetone); IR (ATR, cm^{-1}): 3120 (Ar–CH), 2924 (Aliph. CH), 1592 (C=N); ^{1}H NMR (400 MHz, DMSO-d_6, δ ppm): 3.72 (s, 6H, 2-OCH_3), 4.33 (s, 2H, -CH_2), $(OCH_3)_2$Ar–H [6.93 (q, $J = 12.0$ Hz, 2H), 6.99 (s, 1H)], Phenyl-H [7.57 (d, $J = 8.0$ Hz, 2H), 7.78 (t, $J = 8.0$ Hz, 2H)], Imidazole-H [8.67 (s, 1H)]; ^{13}C NMR (100 MHz, DMSO-d_6, δ ppm): 37.01 (–CH_2), 55.96 (–OCH_3), $(OCH_3)_2$Ar–C [111.14 (CH), 112.48 (CH), 120.52 (CH), 128.52 (C), 148.69 (C), 149.36 (C)], Phenyl-C [121.75 (C), 127.03 (CH), 132.02 (C), 133.65 (CH)], Imidazole-C [113.30 (CH), 145.63 (C)], Thiadiazole-C [144.08 (C), 166.08 (C)]; MS: *m/z* 430.39 (M^+, 60), 432.35 (M+2, 90). Anal. Calcd. for $C_{19}H_{16}BrN_3O_2S$: C, 53.03; H, 3.75; N, 9.76. Found: C, 53.11; H, 3.78; N, 9.79.

*6-(4-Chlorophenyl)-2-(3,4-dimethoxybenzyl)imidazo[2,1-*b*][1,3,4]thiadiazole (**15**)*

Yellow solid, yield 0.94 g (61%), mp 163–165 °C (from Acetone); IR (ATR, cm^{-1}): 3121 (Ar–CH), 2923 (Aliph. CH), 1592 (C=N); ^{1}H NMR (400 MHz, DMSO-d_6, δ ppm): 3.72 (s, 6H, 2-OCH_3), 4.33 (s, 2H, -CH_2), $(OCH_3)_2$Ar-H [6.93 (q, $J = 12.0$ Hz, 2H), 6.99 (s, 1H)], Phenyl-H [7.43 (d, $J = 8.0$ Hz, 2H), 7.84 (d, $J = 8.0$ Hz, 2H)], Imidazole-H [8.66 (s, 1H)]; ^{13}C NMR (100 MHz, DMSO-d_6, δ ppm): 37.01 (–CH_2), 55.95 (-OCH_3), $(OCH_3)_2$Ar–C [111.10 (CH), 112.48 (CH), 121.74 (CH), 129.11 (C), 148.70 (C), 149.36 (C)], Phenyl-C [126.71 (CH), 128.52 (CH), 132.00 (C), 133.29 (C)], Imidazole-C [113.30 (CH), 145.62 (C)], Thiadiazole-C [144.05 (C), 166.04 (C)]; MS: *m/z* 386.21 (M +1, 100). Anal. Calcd. for $C_{19}H_{16}ClN_3O_2S$: C, 59.14; H, 4.18; N, 10.89. Found: C, 59.19; H, 4.15; N, 10.88.

*2-(3,4-Dimethoxybenzyl)-6-(4-fluorophenyl)imidazo[2,1-*b*][1,3,4]thiadiazole (**16**)*

White solid, yield 0.77 g (52%), mp 147–149 °C (from Acetone); IR (ATR, cm^{-1}): 3107 (Ar–CH), 2952 (Aliph. CH), 1594 (C=N); ^{1}H NMR (400 MHz, DMSO-d_6, δ ppm): 3.72 (s, 6H, 2-OCH_3), 4.33 (s, 2H, –CH_2), $(OCH_3)_2$Ar-H [6.91 (q, $J = 12.0$ Hz, 2H), 6.99 (s, 1H)], Phenyl-H [7.22 (dd, $J = 8.0$, 4.0 Hz, 2H), 7.85 (dd, $J = 8.0$, 4.0 Hz, 2H)], Imidazole-H [8.60 (s, 1H)]; ^{13}C NMR (100 MHz, DMSO-d_6, δ ppm): 36.99 (-CH_2), 55.96 (-OCH_3), $(OCH_3)_2$Ar-C [110.53 (CH), 112.48 (CH), 121.74 (CH), 128.56 (C), 148.68 (C), 149.36 (C)], Phenyl-C [116.07 (CH), 127.00 (CH), 130.93 (C), 160.65 (C)], Imidazole-C [113.29 (CH), 145.42 (C)], Thiadiazole-C [144.34 (C), 165.81 (C)]; MS: *m/z* 369.86 (M^+, 100). Anal. Calcd. for $C_{19}H_{16}FN_3O_2S$: C, 61.77; H, 4.37; N, 11.37. Found: C, 61.65; H, 4.39; N, 11.42.

*2-(3,4-Dimethoxybenzyl)-6-(4-methoxyphenyl)imidazo[2,1-*b*][1,3,4]thiadiazole (**17**)*

Yellow crystals, yield 0.95 g (62%), mp 167–169 °C (from Acetone); IR (ATR, cm^{-1}): 3115 (Ar–CH), 2943 (Aliph. CH), 1595 (C=N); ^{1}H NMR (400 MHz, DMSO-d_6, δ ppm): 3.73 (s, 6H, 2-OCH_3), 3.75 (s, 3H, –OCH_3), 4.32 (s, 2H, -CH_2), $(OCH_3)_2$Ar-H [6.92–6.88 (m, 2H), 6.99 (d, $J = 8.0$ Hz, 1H)], Phenyl-H [6.95 (dd, $J = 4.0$, 2.0 Hz, 2H), 7.75 (dd, $J = 8.0$, 4.0 Hz, 2H)], Imidazole-H [8.48 (s, 1H)]; ^{13}C NMR (100 MHz, DMSO-d_6, δ ppm): 36.98 (-CH_2), 55.56 (–OCH_3), 55.96 (–OCH_3), $(OCH_3)_2$Ar–C [109.50 (CH), 112.48 (CH), 121.71 (CH), 128.63 (C), 148.68 (C), 149.36 (C)], Phenyl-C [114.51 (CH), 126.38 (C), 127.03 (CH), 159.08 (C)], Imidazole-C [113.28 (CH), 145.31 (C)], Thiadiazole-C [145.08 (C), 165.25 (C)]; MS: *m/z* 382.23 (M +1, 100). Anal. Calcd. for $C_{20}H_{19}N_3O_3S$: C, 62.97; H, 5.02; N, 11.02. Found: C, 62.91; H, 5.05; N, 11.10.

*2-(3,4-Dimethoxybenzyl)-6-(4-nitrophenyl)imidazo[2,1-*b*][1,3,4]thiadiazole (**18**)*

Yellow solid, yield 0.92 g (58%), mp 174–176 °C (from Acetone); IR (ATR, cm^{-1}): 3115 (Ar–CH), 2926 (Aliph. CH), 1591 (C=N), 1514, 1335 (–NO_2); ^{1}H NMR (400 MHz, DMSO-d_6, δ ppm): 3.73 (s, 6H, 2-OCH_3), 4.33 (s, 2H, –CH_2), $(OCH_3)_2$Ar-H [6.93 (q, $J = 12.0$ Hz, 2H), 7.00 (s, 1H)], Phenyl-H [8.09 (d, $J = 8.0$ Hz, 2H), 8.25 (d, $J = 8.00$ Hz, 2H)], Imidazole-H [8.92 (s, 1H)]; ^{13}C NMR (100 MHz, DMSO-d_6, δ ppm): 36.99 (–CH_2), 55.96 (-OCH_3), $(OCH_3)_2$Ar–C [110.53 (CH), 112.48 (CH), 121.74 (CH), 129.10 (C), 148.69 (C), 149.36 (C)], Phenyl-C [124.69 (CH), 125.71 (CH), 140.85 (C), 146.57 (C)], Imidazole-C [113.61 (CH)], 143.42 (C)], Thiadiazole-C [144.34 (C),

165.81 (C)]; MS: *m/z* 396.94 (M^+, 100). Anal. Calcd. for $C_{19}H_{16}N_4O_4S$: C, 57.57; H, 4.07; N, 14.13. Found: C, 57.62; H, 4.15; N, 14.18.

*4-(2-(3,4-Dimethoxybenzyl)imidazo[2,1-b][1,3,4] thiadiazol-6-yl)benzonitrile (**19**)*

White solid, yield 0.98 g (65%), mp 170–172 °C (from Acetone); IR (ATR, cm^{-1}): 3090 (Ar–CH), 2940 (Aliph. CH), 2228 (C≡N), 1575 (C=N); ^{1}H NMR (400 MHz, DMSO-d_6, δ ppm): 3.72 (s, 6H, 2-OCH_3), 4.34 (s, 2H, –CH_2), $(OCH_3)_2$Ar–H [6.92 (q, $J = 12.0$ Hz, 2H), 6.99 (s, 1H)], Phenyl-H [7.84 (d, $J = 8.0$ Hz, 2H), 8.00 (d, $J = 8.0$ Hz, 2H)], Imidazole-H [8.84 (s, 1H)]; ^{13}C NMR (100 MHz, DMSO-d_6, δ ppm): 37.03 (-CH_2), 55.97 (-OCH_3), $(OCH_3)_2$Ar-C [109.68 (CH), 112.47 (CH), 121.77 (CH), 128.42 (C), 148.71 (C), 149.37 (C)], Phenyl-C [112.85 (C), 125.51 (CH), 133.18 (CH), 138.88 (C)], 119.48 (C≡N), Imidazole-C [113.32 (CH), 146.24 (C)], Thiadiazole-C [143.39 (C), 166.80 (C)]; MS: *m/z* 376.86 (M^+, 100). Anal. Calcd. for $C_{20}H_{16}N_4O_2S$: C, 63.81; H, 4.28; N, 14.88. Found: C, 63.87; H, 4.33; N, 14.91.

*6-([1,1′-Biphenyl]-4-yl)-2-(3,4-dimethoxybenzyl)imidazo [2,1-b][1,3,4]thiadiazole (**20**)*

Gray solid, yield 1.01 g (59%), mp 167–169 °C (from Acetone); IR (ATR, cm^{-1}): 3123 (Ar–CH), 2919 (Aliph. CH), 1592 (C=N); ^{1}H NMR (400 MHz, DMSO-d_6, δ ppm): 3.73 (s, 6H, 2-OCH_3), 4.33 (s, 2H, –CH_2), $(OCH_3)_2$Ar–H [6.93 (q, $J = 12.0$ Hz, 2H), 6.99 (s, 1H)], Phenyl-H [7.69 (d, $J = 8.0$ Hz, 2H), 7.92 (d, $J = 8.0$ Hz, 2H)], Phenyl-Phenyl-H [7.25 (t, $J = 12.0$ Hz, 1H), 7.38 (t, $J = 12.0$ Hz, 2H), 7.83 (d, $J = 8.0$ Hz, 2H)], Imidazole-H [8.61 (s, 1H)]; ^{13}C NMR (100 MHz, DMSO-d_6, δ ppm): 37.00 (-CH_2), 55.96 (–OCH_3), $(OCH_3)_2$Ar–C [110.67 (CH), 112.48 (CH), 121.74 (CH), 129.08 (C), 148.68 (C), 149.37 (C)], Phenyl-C [125.05 (CH), 127.66 (CH), 128.57 (C), 134.37 (C)], Imidazole-C [113.30 (CH), 145.38 (C)], Phenyl-Phenyl-C [125.59 (CH), 126.90 (CH), 127.34 (CH), 129.39 (C)], Thiadiazole-C [145.25 (C), 165.75 (C)]; MS: *m/z* 428.17 (M +1, 100). Anal. Calcd. for $C_{25}H_{21}N_3O_2S$: C, 70.24; H, 4.95; N, 9.83. Found: C, 70.21; H, 4.99; N, 9.78.

*2-(3,4-Dimethoxybenzyl)-6-(naphthalen-2-yl)imidazo[2,1-b][1,3,4]thiadiazole (**21**)*

White solid, yield 0.98 g (61%), mp 192–193 °C (from Acetone); IR (ATR, cm^{-1}): 3059 (Ar–CH), 2984 (Aliph. CH), 1590 (C=N); ^{1}H NMR (400 MHz, DMSO-d_6, δ ppm): 3.73 (s, 6H, 2-OCH_3), 4.35 (s, 2H, –CH_2), $(OCH_3)_2$Ar–H [6.94 (q, $J = 12.0$ Hz, 2H), 7.01 (s, 1H)])], Naphthyl-H [7.51–7.44 (m, 2H), 7.93–7.87 (m, 3H), 7.98 (t, $J = 12.0$ Hz, 1H), 8.37 (s, 1H)], Imidazole-H [8.77 (s, 1H)]; ^{13}C NMR (100 MHz, DMSO-d_6, δ ppm): 37.03 (-CH_2), 55.98 (–OCH_3), $(OCH_3)_2$Ar–C [111.24 (CH), 112.50 (CH), 121.78 (CH), 128.61 (C), 148.70 (C), 149.37 (C)], Naphtyl-C [123.11 (CH), 123.85 (CH), 126.22 (CH), 126.90 (CH), 128.07 (CH), 128.35 (CH), 128.57 (CH), 131.84 (C), 132.79 (C), 133.68 (C)], Imidazole-C [113.32 (CH), 145.68 (C)], Thiadiazole-C [145.22 (C), 165.90 (C)]; MS: *m/z* 401.99 (M^+, 100). Anal. Calcd. for $C_{23}H_{19}N_3O_2S$: C, 68.81; H, 4.77; N, 10.47. Found: C, 68.85; H, 4.74; N, 10.41.

Biological activity

In vitro effect of the compounds against plant pathogens

The antifungal activity of the compounds was determined by the agar well diffusion method (Garammar 1976). Different concentrations (5, 2.5, 1.25 and 0.625 mg/mL) of compounds were obtained after they were dissolved in DMSO. DMSO was used (100 µL/well) as a negative control. A commercial dose of Thiram 80% was used as a positive control. The PDA was poured into 90 mm petri plates (~20 mL/plate^{-1}). Four (5 mm diameter) wells were opened by a sterile cork borer at a position of 30 mm from the centre on the PDA plate. Each plate contained four different concentrations (5, 2.5, 1.25, and 0.625 mg/mL) of all compounds. Each dose (100 µL/well) was added to the well and kept at room temperature for 2 h during the diffusion period. The PDA plates were incubated (in the centre of the PDA) with 5 mm plugs from seven-day-old cultures. The plates were then incubated at 22 ± 2 °C for 7 d. The experiment was designed with three replicates and repeated two times. All inhibition zones were recorded. All antifungal activity values were determined by measuring the inhibition zone diameter between the pathogen and the well. The percentage of inhibition was calculated according to the following formula; (Vyas et al. 2006)

$$\%\ \text{Inhibition} = \text{Inhibition zone in treatment}/\text{Control}* \text{ x } 100$$

*Control: Mycelial growth of negative control

Acknowledgements The financial support under the contract (KBÜ-BAP-15/2-YL-017) from Karabük University is gratefully acknowledged.

Compliance with Ethical Standards

Conflict of Interest The authors declare that they have no conflict of interest.

References

Alegaon SG, Alagawadi KR, Sonkusare PV, Chaudhary SM, Dadwe DH, Shah AS (2012) Novel imidazo[2,1-b][1,3,4]thiadiazole

carrying rhodanine-3-acetic acid as potential antitubercular agents. Bioorg Med Chem Lett 22:1917–1921
Alegaon SG, Alagawadi KR (2011) Synthesis, characterization and antimicrobial activity evaluation of new imidazo[2,1-b][1,3,4] thiadiazole derivatives. Eur J Chem 2:94–99
Alwan WS, Karpoormath R, Palkar MB, Patel HM, Rane RA, Shaikh MS, Kajee A, Mlisina KP (2015) Novel imidazo[2,1-b]-1,3,4-thiadiazoles as promising antifungal agents against clinical isolate of Cryptococcus neoformans. Eur J Med Chem 95:514–525
Atta KFM, Farahat OOM, Ahmed AZA, Marai MG (2011) Synthesis and antibacterial activities of novel imidazo[2,1-b]-1,3,4-thiadiazoles. Molecules 16:5496–5506
Bakherad M, Keivanloo A, Tajbakhsh M, Kamali TA (2010) Synthesis of 6-benzylimidazo[2,1-b][1,3]thiazole during sonogashira coupling. Synth Commun 40:173–178
Banu A, Lamani RS, Khazi IM, Begum NS (2010) Synthesis and Crystal Structure of 2-(4-Fluorobenzyl)-6-Phenylimidazo[2,1-b][1,3,4] Thiadiazole-5-Carbaldehyde. Mol Cryst Liq Cryst 533:141–151
Bruker (2008) APEX2 and SAINT. Bruker AXS Inc., Madison, WI
Chandrakantha B, Isloor AM, Shetty P, Fun HK, Hedge G (2014) Synthesis and biological evaluation of novel substituted 1,3,4-thiadiazole and 2,6-di aryl substituted imidazo [2,1-b] [1,3,4] thiadiazole derivatives. Eur J Med Chem 71:316–323
Copin C, Henry N, Buron F, Routier S (2012) Synthesis of 2,6-disubstituted imidazo[2,1-b][1,3,4]thiadiazoles through cyclization and suzuki–miyaura cross-coupling reactions. Eur J Org Chem 2012: 6804–6806
Dolomanov OV, Bourhis LJ, Gildea RJ, Howard JAK, Puschmann H (2009) A complete structure solution, refinement and analysis program. J Appl Cryst 42:339–341
Ece A, Sevin F (2013) The discovery of potential cyclin A/CDK2 inhibitors: a combination of 3D QSAR pharmacophore modeling, virtual screening, and molecular docking studies. Med Chem Res 22(12):5832–5843
El-Gohary NS, Shaaban MI (2013) Synthesis, antimicrobial, anti-quorum-sensing, antitumor and cytotoxic activities of new series of fused [1,3,4]thiadiazoles. Eur J Med Chem 63:185–195
Er M, Isildak G, Tahtaci H, Karakurt T (2016) Novel 2-amino-1,3,4-thiadiazoles and their acyl derivatives: Synthesis, structural characterization, molecular docking studies and comparison of experimental and computational results. J Mol Struct 1110:102–113
Er M, Şahin A, Tahtaci H (2014) Synthesis and characterization of novel 1,3-thiazole and 2-amino-1,3,4-thiadiazole derivatives. Maced J Chem Chem Eng 33:189–198
Friesner RA, Banks JL, Murphy RB, Halgren TA, Klicic JJ, Mainz DT, Repasky MP, Knoll EH, Shaw DE, Shelley M, Perry JK, Francis P, Shenkin PS (2004) Glide: A new approach for rapid, accurate docking and scoring. 1. method and assessment of docking accuracy. J Med Chem 47:1739–1749
Friesner RA, Murphy RB, Repasky MP, Frye LL, Greenwood JR, Halgren TA, Sanschagrin PC, Mainz DT (2006) Extra precision glide: docking and scoring incorporating a model of hydrophobic enclosure for protein-ligand complexes. J Med Chem 49:6177–6196
Gadad AK, Palkar MB, Anand K, Noolvi MN, Boreddy TS, Wagwade J (2008) Synthesis and biological evaluation of 2-trifluoromethyl/sulfonamido-5,6-diaryl substituted imidazo[2,1-b]-1,3,4-thiadiazoles: A novel class of cyclooxygenase-2 inhibitors. Bioorg Med Chem 16:276–283
Garammar A (1976) Antibiotic sensitivity and assay test. In: Collins CH, Lyne PM, Grange JM (Eds.) micro-biological methods. Bulterworths and Co. Ltd., London, p 235
Halgren TA, Murphy RB, Friesner RA, Beard HS, Frye LL, Pollard WT, Banks JL (2004) Glide: a new approach for rapid, accurate docking and scoring. 2. enrichment factors in database screening. J Med Chem 47:1750–1759
Harder E, Damm W, Maple J, Wu C, Reboul M, Xiang JY, Wang L, Lupyan D, Dahlgren MK, Knight JL, Kaus JW, Cerutti DS, Krilov G, Jorgensen WL, Abel R, Friesner RA (2015) Opls3: a force field providing broad coverage of drug-like small molecules and proteins. J Chem Theory Comput 2015, doi:10.1021/acs.jctc.5b00864
Jadhav VB, Kulkarni MV, Rasal VP, Biradar SS, Vinay MD (2008) Synthesis and anti-inflammatory evaluation of methylene bridged benzofuranyl imidazo[2,1-b][1,3,4]thiadiazoles. Eur J Med Chem 43:1721–1729
Jalhan S, Jındal A, Gupta A, Hemraj (2012) Synthesis, biological activities and chemistry of thiadiazole derivatives and schiff bases. Asian J Pharm Clin Res 5:199–208
Kadi AA, El-Brollosy NR, Al-Deeb OA, Habib EE, Ibrahim TM, El-Emam AA (2007) Synthesis, antimicrobial, and anti-inflammatory activities of novel 2-(1-adamantyl)-5-substituted-1,3,4-oxadiazoles and 2-(1-adamantylamino)-5-substituted-1,3,4-thiadiazoles. Eur J Med Chem 42:235–242
Kamal A, Reddy VS, Santosh K, Kumar GB, Shaik AB, Mahesh R, Chourasiya SS, Sayeed IB, Kotamraju S (2014) Synthesis of imidazo[2,1-b][1,3,4]thiadiazole–chalcones as apoptosis inducing anticancer agents. Med Chem Commun 5:1718–1723
Karki SS, Panjamurthy K, Kumar S, Nambiar M, Ramareddy SA, Chiruvella KK, Raghavan C (2011) Synthesis and biological evaluation of novel 2-aralkyl-5-substituted-6-(4'-fluorophenyl)-imidazo[2,1-b][1,3,4]thiadiazole derivatives as potent anticancer agents. Eur J Med Chem 46:2109–2116
Kim HS, Jadhav JR, Jung SJ, Kwak JH (2013) Synthesis and antimicrobial activity of imidazole and pyridine appended cholestane-based conjugates. Bioorg Med Chem Lett 23:234315–4318
Kotha S, Lahiri K, Kashinath D (2002) Recent applications of the Suzuki–Miyaura cross-coupling reaction in organic synthesis. Tetrahedron 58:9633–9695
Kumar S, Hedge M, Gopalakrishnan V, Renuka VK, Ramareddy SA, De Clercq E, Schols D, Narasimhamurthy AKG, Raghavan SC, Karki SS (2014) 2-(4-Chlorobenzyl)-6-arylimidazo[2,1-b][1,3,4] thiadiazoles: Synthesis, cytotoxic activity and mechanism of action. Eur J Med Chem 84:687–697
Lamani RS, Shetty NS, Kamble RR, Khazi IAM (2009) Synthesis and antimicrobial studies of novel methylene bridged benzisoxazolyl imidazo[2,1-b][1,3,4]thiadiazole derivatives. Eur J Med Chem 44:2828–2833
Lata, Kushwaha K, Gupta A, Meena D, Verma A (2015) Biological activities of imidazo[2,1-b][1,3,4]thiadiazole derivatives: a review. Heterocycl Lett 5:489–509
Luo Y, Zhang S, Liu ZJ, Chen W, Fu J, Zeng QF, Zhu HL (2013) Synthesis and antimicrobical evaluation of a novel class of 1,3,4-thiadiazole: Derivatives bearing 1,2,4-triazolo[1,5-a] pyrimidine moiety. Eur J Med Chem 64:54–61
Mascarenhasa NM, Ghoshal N (2008) An efficient tool for identifying inhibitors based on 3D-QSAR and docking using feature-shape pharmacophore of biologically active conformation-A case study with CDK2/CyclinA. Eur J Med Chem 43(12):2807–2818
Noolvi MN, Patel HM, Kamboj S, Kaur A, Mann V (2012) 2,6-Disubstituted imidazo[2,1-b][1,3,4]thiadiazoles: Search for anticancer agents. Eur J Med Chem 56:56–69
Noolvi MN, Patel HM, Singh N, Gadad AK, Cameotra SS, Badiger A (2011) Synthesis and anticancer evaluation of novel 2-cyclopropylimidazo[2,1-b][1,3,4]-thiadiazole derivatives. Eur J Med Chem 46:4411–4418
Padmavathi V, Kumari CP, Venkatesh BC, Padmaja A (2011) Synthesis and antimicrobial activity of amido linked pyrrolyl and pyrazolyl-oxazoles, thiazoles and imidazoles. Eur J Med Chem 46:5317–5326

Patel HM, Sing B, Bhardwaj V, Palkar M, Shaikh MS, Rane R, Alwan WS, Gadad AK, Noolvi MN, Karpoormath R (2015) Design, synthesis and evaluation of small molecule imidazo[2,1-b][1,3,4] thiadiazoles as inhibitors of transforming growth factor-b type-I receptor kinase (ALK5). Eur J Med Chem 93:599–613

Ramprasad J, Nayak N, Dalimba U, Yogeeswari P, Sriram D (2015) One-pot synthesis of new triazole-Imidazo[2,1-b][1,3,4]thiadiazole hybrids via click chemistry and evaluation of their antitubercular activity. Bioorg Med Chem Lett 25:4169–4173

Ramprasad J, Nayak N, Dalimba U, Yogeeswari P, Sriram D, Peethambar SK, Achur R, Kumar HSS (2015) Synthesis and biological evaluation of new imidazo[2,1-b][1,3,4]thiadiazole-benzimidazole derivatives. Eur J Med Chem 95:49–63

Romagnoli R, Baraldi PG, Prencipe F, Balzarini J, Liekens S, Estevez F (2015) Design, synthesis and antiproliferative activity of novel heterobivalent hybrids based on imidazo[2,1-b][1,3,4]thiadiazole and imidazo[2,1-b][1,3]thiazole scaffolds. Eur J Med Chem 101:205–217

Sancak K, Ünver Y, Er M (2007) Synthesis of 2-acylamino, 2-aroylamino and ethoxycarbonyl imino-1,3,4-thiadiazoles as antitumor agents. Turk J Chem 31:125–134

Schrödinger Release 2016-4 (2016a) Maestro. Schrödinger, LLC, New York, NY

Schrödinger Release 2016-4 (2016b) QikProp. Schrödinger, LLC, New York, NY

Sheldrick GM (2015) Shelxt-integrated space-group and crystal-structure determination. Acta Cryst A71:3–8

Sheldrick GM (2015) Crystal structure refinement with SHELXL. Acta Cryst C71:3–8

Singh SJ, Rajamanickam S, Gogoi A, Patel BK (2016) Synthesis of 2-amino-substituted-1,3,4-thiadiazoles via 2,3-dichloro-5,6-dicyano-1,4-benzoquinone (DDQ) mediated intramolecular C–S bond formation in thiosemicarbazones. Tetrahedron Lett 57:1044–1047

Tegginamath G, Kamble RR, Taj T, Kattimani PP, Meti GY (2013) Synthesis of novel imidazo[2,1-b][1,3,4]thiadiazoles appended to sydnone as anticancer agents. Med Chem Res 22:4367–4375

Terzioglu N, Gursoy A (2003) Synthesis and anticancer evaluation of some new hydrazone derivatives of 2,6-dimethylimidazo[2,1-b] [1,3,4]thiadiazole-5-carbohydrazide. Eur J Med Chem 38:781–786

Tzitzikas TZ, Neochoristis CG, Stephanatou JS, Tsoleridis CA, Buth G, Kostakis GE (2013) Azodicarboxylates: valuable reagents for the multicomponent synthesis of novel 1,3,4-thiadiazoles and imidazo[2,1-b][1,3,4]thiadiazoles. Tetrahedron 69:5008–5015

Vyas YK, Bhatnagar M, Sharma KJ (2006) Antimicrobial activity of a herb, herbal based and synthetic dentifrices against oral microflora. J Cell Tissue Res 6:639–642